

Laboratory-Prostate cancer

Programmed death ligand 1 expression in prostate cancer cells is associated with deep changes of the tumor inflammatory infiltrate composition

Manuel Scimeca, PhD^{a,b,c}, Rita Bonfiglio, PhD^d, Nicoletta Urbano, RPh, BCNP^{e,§}, Chiara Cerroni, BSc^a, Lucia Anemona, MD^a, Manuela Montanaro, BSc^a, Sara Fazi, BSc^a, Orazio Schillaci, MD, PhD^{b,f}, Alessandro Mauriello, MD^a, Elena Bonanno, MD, PhD^{a,g,*},¹

^a Department of Biomedicine and Prevention, University of Rome "Tor Vergata", Rome, Italy

^b San Raffaele University, Rome, Italy

^c OrchideaLab S.r.l., Rome, Italy

^d Department of Experimental Medicine and Surgery, University "Tor Vergata", Rome, Italy

^e Nuclear Medicine, Policlinico "Tor Vergata", Rome, Italy

^f IRCCS Neuromed, Pozzilli, Italy

^g "Diagnostica Medica" and "Villa dei Platani", Avellino, Italy

Received 14 August 2018; received in revised form 12 February 2019; accepted 18 February 2019

Abstract

Background: The main aim of this study was to investigate the putative correlation between the composition of intratumoral inflammatory infiltrate and the expression of programmed death ligand 1 (PD-L1) by prostate cancer cells. In addition, we evaluated the correlation between the expression of PD-L1 and PTX3.

Methods: We enrolled 100 patients from which we collected one surgical sample each. Paraffin serial sections were obtained to perform histological classifications and tissues microarray construction. Serial tissues microarray paraffin sections were also used for PD-L1 analysis and intratumoral inflammatory infiltrate characterization (CD4, CD8, CD57, CD3, PD1, PSGL-1, TIGIT, CD20, CD38, CD68, CD163, and PTX3) by immunohistochemistry.

Results: Our result showed a significant increase of the number of both PD-L1 and PTX3 positive cells in prostate tumors respect to benign lesions. Inflammatory infiltrate of PD-L1 positive prostate cancer lesions was characterized by a decrease of both PD1 positive lymphocytes and tumor-infiltrated macrophages, mainly M2 subpopulation. Also, PTX3 expression showed an inverse correlation with the number of PD-L1 positive prostate cancer cells.

Conclusions: If confirmed, our data could be useful to predict the variations of the inflammatory population related to PD-L1 expression in prostate cancer. This can lay the foundation to establish therapeutic protocols able to inhibit the PD-L1 activity and, at the same time, to reactivate the antitumor inflammatory process. © 2019 Elsevier Inc. All rights reserved.

Keywords: PD-L1; Cancer immune-escape; Prostate cancer; Macrophages; M2 polarization; PTX3

1. Introduction

Prostate cancer (PC) is the second most commonly diagnosed malignant tumor in men and a major cause of mortality, with an estimated 385,560 deaths globally expected in 2020 [1]. Different types of treatment are available for patients with prostate cancer. Briefly, watchful waiting and active surveillance are recommended for older patients who

*Corresponding author. Tel.: + 390620903913.

E-mail address: elena.bonanno@uniroma2.it (E. Bonanno).

§Manuel Scimeca, Rita Bonfiglio, and Nicoletta Urbano equally first authors.

¹Orazio Schillaci, Alessandro Mauriello, and Elena Bonanno equally last authors.

do not have signs or symptoms of advance cancer progression. Conversely, prostatectomy represent the main option for patients in good health with a local prostate cancer lesion [2,3]. Patients with high-grade prostate cancer, metastatic lesions, or biochemical recurrence generally undergo to hormonal and radiation therapy [3]. Although it can be very effective for *recurrent* disease, patients usually become refractory to hormonal therapy (castration resistant) within 1 to 3 years [3]. This is usually associated with the transition to a more aggressive status of the disease, leading to the development of distant metastases [4]. In the last few years, the identification and the approval of several agents for the treatment of metastatic prostate cancer, including cytotoxic drugs (cabazitaxel) [5], radiopharmaceuticals, and second-generation antiandrogen compounds (abiraterone acetate and enzalutamide) [6,7] have rapidly changed the management of prostate cancer patients [8].

It is known that prostate cancer progression results from a tumor-induced immunosuppressive status, in which the immune system is not able to identify and destroy cancer cells since they are able to elude the antitumor immune response [8]. Thus, immune evasion is now considered as a hallmark of cancer [9]. In this context, immune checkpoints play a prominent role in cancer immune escape. Indeed, immune checkpoint pathways dampen T-cell activity physiologically, being crucial for minimizing inflammatory-dependent tissue damage and the maintenance of self-tolerance [8]. An important mechanism of cancer immune escape involves interaction between the programmed death 1 (PD-1) receptor on cytotoxic T lymphocytes (CTLs) with the programmed death ligand 1 (PD-L1) on cancer cells or other host immune cells [10]. The PD-1/PD-L1 axis is one of several immune checkpoint regulators that have physiological roles in self-tolerance and in limiting the duration and amplitude of immune responses, primarily through the inhibition of adaptive T-cell responses [11]. PD-1 is a cell surface protein belonging to the B7 co-stimulatory factor family [12].

PD-L1 expression has been studied in different malignant cancers, including lung, kidney, oesophagus, prostate, and colorectal cancer with the evidence of correlation with poor patient prognosis [12]. These studies demonstrate that the expression of PD-L1 make tumor cells able to elude cancer immunosurveillance [12]. Based on these evidences, new emerging anti-PD-L1 immunotherapies are now attempting to contrast cancer by initiating or augmenting T-cell responses against tumor cells. Nevertheless, even though promising results have been achieved, the effective prognostic and predictive value of PD-L1 expression in prostate cancer cells is not clear yet. In this scenario, the identification of new molecules involved in the immune-escape of prostate cancer, as well as their interaction with the PD-1/PD-L1 checkpoint, can improve our knowledge about the biology of tumor progression. In the last years, several studies highlighted the dual role of PTX3 in tumor progression. PTX3, also known as TSG-14, was firstly

described in 1992 as the prototypic member of the long-pentraxin subfamily [13]. PTX3 is released by peripheral blood leukocytes and myeloid dendritic cells in response to proinflammatory stimuli (such as $\text{TNF}\alpha$ and $\text{IL1}\beta$) by acting as a nonredundant component of the humoral arm of the innate immunity and as an essential player in tuning inflammation [14]. Although there are several studies reporting the effect of PTX3 on cancer biology, the role of PTX3 in cancer remains unclear. Overexpression of PTX3 in tumor tissues was considered as an unfavorable prognostic factor in the setting of pancreatic carcinoma [15], head and neck squamous cell carcinoma [16], gastric cancer [17], breast cancer [18,19], glioma [20], prostate cancer [21,22], and lung cancer [23]. On the contrary, PTX3 was found downregulated and played an antitumoral activity in melanoma [24] and esophageal carcinoma [25]. In addition, a role of PTX3 in inflammatory-related carcinogenesis has been described [26]. Thus, PTX3 expression by both prostate cancer cells and inflammatory infiltrate, especially macrophages, could represent a further element in the complex mechanism of prostate cancer progression.

The main aim of this study was to investigate the putative correlation between the composition of intratumoral inflammatory infiltrate and the expression of PD-L1 by prostate cancer cells. In addition, we evaluated the correlation between the expression of PD-L1 and PTX3.

2. Materials and methods

2.1. Prostate samples collection

In this retrospective study, we enrolled 100 patients from which we collected one prostate biopsy each. Exclusion criteria were: history of previously or concomitant other neoplastic diseases, autoimmune diseases, viral chronic infections (HBV, HCV, HIV), any antitumoral treatment received before biopsy. The Independent Ethical Committee of “Policlinico Tor Vergata” approved our study protocol. All experimental procedures were carried out according to The Code of Ethics of the World Medical Association (Declaration of Helsinki). Informed consent was obtained from all patients prior to surgery. Specimens were handled and carried out in accordance with the approved guidelines.

From surgical sample, paraffin serial sections were obtained to perform histological classifications and tissues microarray (TMA) construction. Serial TMA paraffin sections were used for PD-L1 analysis and intratumoral inflammatory infiltrate characterization by immunohistochemistry.

2.2. Histology

After fixation in 10% buffered formalin for 24 hours, prostate tissues were paraffin embedded. About 4- μm thick sections were stained with hematoxylin and eosin [27].

2.3. TMA construction

For TMA construction, we utilized fragments of tissues left over the sampling procedures for diagnostic purposes. Areas of interest from 50 PC and 50 prostate benign lesions (BL) were identified in corresponding hematoxylin and eosin-stained sections and marked on the donor paraffin block. A 3.14 mm²-cross section of the donor block was placed in the recipient master block of the Galileo TMA CK2500 (Brugherio, Milan, Italy). Three cores from different areas of the same tissue block (9.42 mm² cross section) were arrayed for each case (total amount of neoplastic cells not less than 500) [28].

2.4. Immunohistochemistry

We employed immunohistochemical techniques to study the expression of PD-L1 and PTX3 in prostate cells and the expression of CD4, CD8, CD57, CD3, PD1, PSGL-1, TIGIT, CD20, CD38, CD68, and CD163 to characterize intratumoral inflammatory infiltrate.

Briefly, antigen retrieval was performed on 4 μm-thick paraffin sections using EDTA citrate pH 7.8 or Citrate pH 6.0 buffers for 30 min at 95°C. Sections were then incubated for 1 hour at room temperature with primary antibodies (listed in Table 1). Washings were performed with PBS/Tween20 pH 7.6. Reactions were revealed by HRP - DAB Detection Kit (UCS Diagnostic, Rome, Italy).

All markers (PD-L1, PTX3, CD4, CD8, PD1, PSGL-1, TIGIT, CD57, CD3, CD20, CD38, CD68, and CD163) were evaluated with the support of a digital software (ImageViewer, Ventana, Roche) by two blind observers by counting the number of positive prostate cells on 9.42 mm² prostate tissues. For the analysis of macrophage populations (CD68, CD38, and CD163), we did not consider as positive those cells with morphological appearance of both B and T cells. Results were reported as number of positive cells on 1 mm² of tissues (Mean ± SEM).

2.5. Statistical analysis

In order to forego assumptions of data normality, we conducted group-wise comparisons (see below for definition of the three groups analyzed) of biomarker values through nonparametric Kruskal-Wallis (KW) tests followed by pairwise comparison (Conover's-test for multiple comparisons) whenever the result of the KW test was statistically significant ($P < 0.05$). Results of post-hoc testing were corrected for multiple comparisons using a false discovery rate procedure ($\alpha = 0.05$).

3. Results

3.1. Histological classification

The study of H&E sections allowed us to classify prostate biopsies according to EAU-ESTRO-SIOG Guidelines

Table 1
List of primary antibodies

Antibody	Characteristics	Dilution	Retrieval	Target
anti-PD-L1/CD274	Rabbit monoclonal clone QR1; Quartett, Schichauweg 16, 12307 Berlin, Germany	1:100	EDTA citrate pH 7.8	Cancer cells, T Lymphocytes, Macrophages and pro-B cells [11]
Anti-CD3	Rabbit monoclonal, clone 2GV6, Ventana, Tucson, AZ, USA	Pre-diluted	EDTA citrate pH 7.8	T Lymphocytes [53]
anti-CD4	Rabbit clone SP37; Ventana, Tucson, AZ, USA	Prediluted	EDTA citrate pH 7.8	T helper cells, macrophages, granulocytes [53,54]
anti-CD8	Rabbit monoclonal clone SP35 Ventana, Tucson, AZ, USA	Prediluted	EDTA citrate pH 7.8	T cytotoxic cells [53]
anti-CD57	Rabbit monoclonal, clone NK-1; Ventana, Tucson, AZ, USA	Prediluted	EDTA citrate pH 7.8	Natural Killer cells, Macrophages, B-cells [53]
anti-PD1	Mouse monoclonal clone NAT105; Ventana, Tucson, AZ, USA	Prediluted	EDTA citrate pH 7.8	T cells, pro-B cells [54]
anti-PSGL1	Mouse monoclonal clone PL-1; Thermo Fisher Scientific Inc. Waltham, MA USA	1:150	Citrate pH 6.0	Myeloid cells, stimulated T lymphocytes and endothelial cells [55]
anti-TIGIT	Mouse monoclonal clone clone TG1; Dianova GmbH / Warburgstr. 45 / 20354 Hamburg	1:100	EDTA citrate pH 7.8	T cells and Natural Killer Cells [57]
anti-CD20	Mouse monoclonal clone L26; Ventana, Tucson, AZ, USA	Prediluted	EDTA citrate pH 7.8	B-cells [53]
anti- CD38	Rabbit monoclonal clone SP149; Ventana, Tucson, AZ, USA	Prediluted	EDTA citrate pH 7.8	M1 macrophages, Lymphocytes and B-cells [58]
anti- CD68	Mouse monoclonal clone KP-1; Ventana, Tucson, AZ, USA	Prediluted	EDTA citrate pH 7.8	Monocytes, Macrophages and Osteoclasts [58]
anti- CD163	Mouse monoclonal clone MRQ-26; Ventana, Tucson, AZ, USA	Prediluted	EDTA citrate pH 7.8	Macrophages, M2 macrophages [58]
anti-PTX3	Rat monoclonal clone MNB1; AbCam, Cambridge, UK	1:100	Citrate pH 6.0	Cancer cells [13,14], Macrophages [61], Endothelial cells [61], fibroblasts [61], osteoblasts [67]

Table 2
Baseline characteristics of patients.

	n	Age ≤55	Age ≥55	Gleason ≤6	Gleason 7	Gleason ≥8	PSA (ng ml ⁻¹)
BL	50	22	28	/	/	/	/
PC	50	15	35	24	12	14	1112.07 ± 128.78

2017 [29] in 50 BL (prostate hyperplasia) and 50 PC. As concerned Gleason score, all PC lesions had values equal or superior to 3+3. Specifically, we classified cancer lesions as follow: 24 cases with 3+3 score, 5 cases with 3+4 score, 7 cases with 4+3 score, 10 cases with 4+4 score, 2 cases with 4+5 score and 2 cases with 5+3 score. The main clinical anamnestic data are reported in Table 2.

3.2. PD-L1 and PTX3 expression

We studied the number of PD-L1 and PTX3 positive cells on 9.42 mm² of prostate tissues (results are expressed as number of positive cells/9.42 mm² ± SEM).

As expected, immunohistochemical analysis showed a significant increase of the number of positive PD-L1 cells in PC group as compared to BL (BL 18.11 ± 12.81; PC 137.6 ± 26.24, $P=0.0047$) (Fig. 1A–C). In addition, we observed no significant correlation between the Gleason score and PD-L1 expression. As concern the inflammatory cells, we noted a very low number of PD-L1 positive lymphocytes in both BL and PC lesions (data not shown). As concern the number of PTX3 positive cancer cells, our results displayed a significant increase in PC respect to BL group (BL 151.1 ± 27.68; PC 404.7 ± 16.32, $P < 0.0001$) (Fig. 1D–F).

3.3. Lymphocyte infiltrate evaluation

We characterized lymphocyte intratumoral infiltrate by studying the number of CD3, CD4, CD8, CD57, PD1, PSGL-1, TIGIT, and CD20 positive cells on 9.42 mm² of prostate tissues (results are expressed as number of positive cells/9.42 mm² ± SEM).

As concern the CD3, Mann–Whitney test revealed significant differences between the number of positive lymphocytes in BL and PC (BL 93.66 ± 10.55 vs. PC 291.0 ± 39.23 $P < 0.0001$) (Fig. 1G–I). Similarly, we observed significant difference between BL and PC regarding the number of CD4 positive lymphocytes (T-helper) (BL 18.19 ± 4.18 vs. PC 190.1 ± 37.68 $P < 0.0001$) (Fig. 1J–L). Conversely, no significant difference was detected for the presence of cytotoxic T cells, both CD8 (Fig. 1M–O) or CD57 (Fig. 2A–C) positive cells. (CD8: BL 93.09 ± 10.58 vs. PC 148.20 ± 23.05, $P=0.1595$; CD57: BL 44.31 ± 6.54 vs. PC 48.70 ± 8.39, $P=0.8629$). Indeed, these cells were frequently present also in prostate benign lesions. Our data showed a very low number of PD1 positive

lymphocytes in PC (18.03 ± 3.31) as compared to BL (74.06 ± 17.83) ($P=0.0005$) (Fig. 2D–F).

Also, we noted a significant increase of PSGL-1 positive lymphocytes in BL as compared PC group (BL 85.71 ± 14.38 vs. PC 56.97 ± 6.52 $P < 0.0001$) (Fig. 2G–I). Conversely, as concern the number of TIGIT positive lymphocytes, no significant differences were observed about between BL and PC BL (34.34 ± 5.30 vs. PC 36.48 ± 6.98 $P=0.9833$) (Fig. 2J–L). Finally, we observed a higher B-cells infiltrate (CD20 positive cells) in PC respect to BL (BL 2.75 ± 0.75 vs. PC 35.04 ± 10.50 $P < 0.0001$) (Fig. 2M–O).

3.5. Macrophage infiltrate evaluation

Macrophage intratumoral infiltrate was characterized by studying the number of CD38, CD68, and CD163 positive macrophages on 9.42 mm² of prostate tissues (results are expressed as number of positive cells/9.42 mm² ± SEM).

CD68 analysis was used to identify the number of both M1 and M2 intratumoral macrophages. For the study of M1 population we investigated the expression of CD38. Due to the expression of CD38 in some lymphocytes, the evaluation of CD38 positive macrophages was performed comparing the expression of CD3 and CD20 on serial sections. Specifically, digital images of these markers were simultaneously displayed on high resolution monitor by using Virtuoso software (Ventana Roche). This procedure made possible to distinguish M1 macrophages (CD38 positive) from other cells simultaneously expressing CD38 and CD3 or CD20. M2 cells were identified by studying the expression of CD163. Our results showed a significant increase of CD68 macrophages in PC as compared to BL (BL 107.5 ± 12.51 vs. PC 236.3 ± 27.12 $P < 0.0001$) (Fig. 3A–C). In agreement with the results obtained from CD68 analysis, we also observed an increase of both M1 and M2 macrophages in PC as compared to BL (Fig. 3D–H). Specifically, we displayed a dramatic high number of M2 (CD163) macrophages in PC respect to BL (BL 29.5 ± 7.17 vs. PC 201.6 ± 26.05 $P < 0.0001$) (Fig. 3D,G,H) and, at a lesser extent, an increase of M1 macrophages (CD38) in PC (BL 22.72 ± 3.09 vs. PC 46.10 ± 7.51 $P=0.0408$) (Fig. 3D–F). On note, although both M1 and M2 macrophages increase in PC, these malignant lesions were characterized by M2 polarization phenomenon. Indeed, PC lesions showed an imbalance between M1/M2 ratio ($P < 0.0001$) (Fig. 3D). Conversely, no difference was detected by comparing the number of M1 and M2 macrophages in BL group ($P=0.7862$) (Fig. 3D).

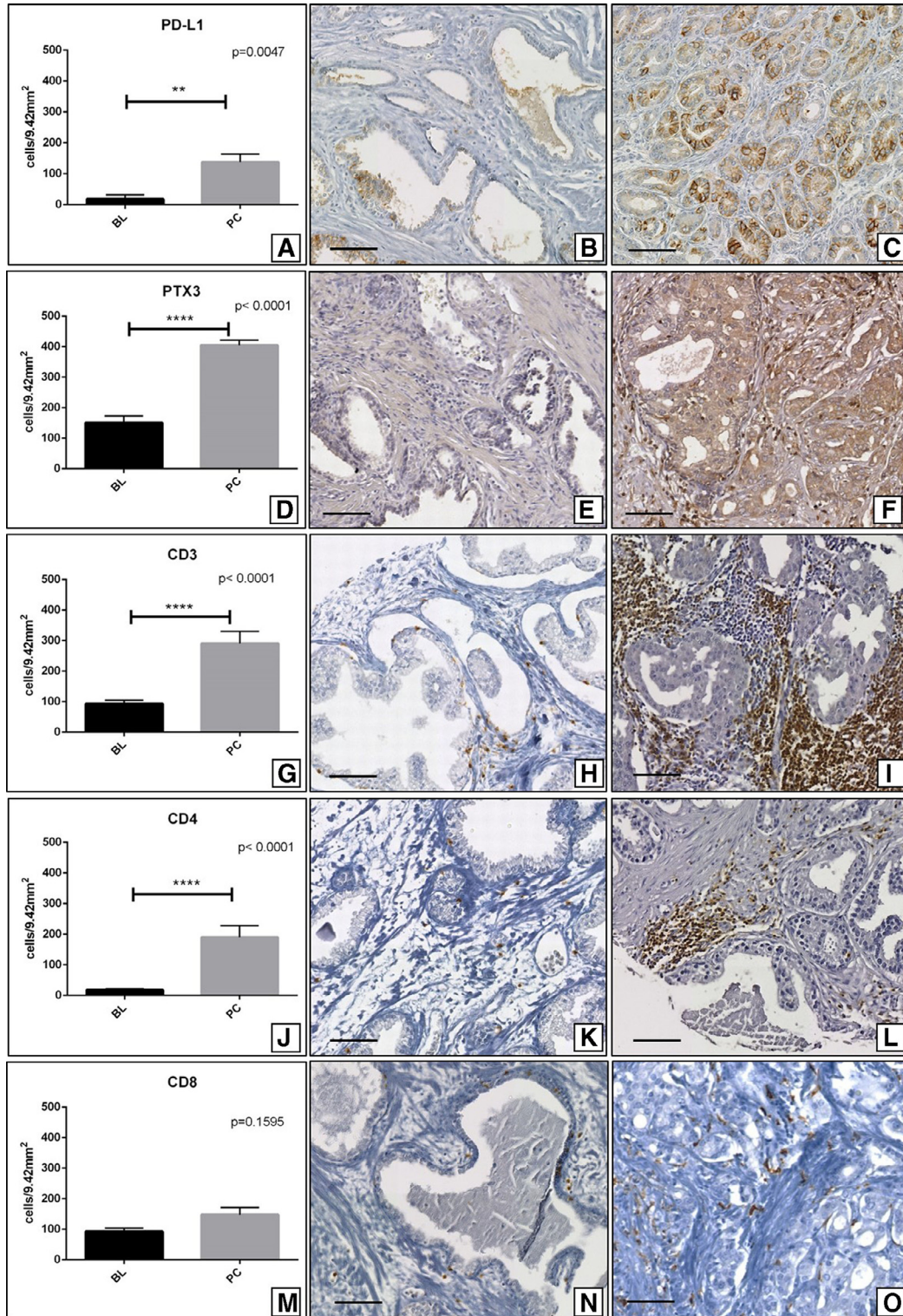


Fig. 1. Evaluation of PD-L1 expression and lymphocyte infiltrate in prostate lesions. (A) Graph shows the number of PD-L1 positive prostate cells in BL and PC lesions. (B) Representative image of PD-L1 expression in BL. (C) Image displays several PD-L1 positive prostate cancer cells. (D) Graph shows the number of PTX3 positive prostate cells in BL and PC lesions. (E) Image displays several PTX3 positive prostate cancer cells. (F) Image displays several PTX3 positive prostate cancer cells. (G) Graph shows the number of CD3 positive cells in BL and PC lesions. (H) Image displays some CD3 positive inflammatory cells in BL. (I) Representative image of tumor-associate inflammatory CD3 positive cells infiltrate in PC. (J) Graph shows the number of CD4 positive cells in BL and PC lesions. (K) No/rare positive CD4 positive cells in BL. (L) Image shows numerous CD4 positive inflammatory cells in PC. (M) Graph shows the number of CD8 positive cells in BL and PC lesions. (N) No/rare positive CD8 positive cells in BL. (O) Representative image of tumor-associate inflammatory CD8 positive cells infiltrate in PC. (Scale bar represents 200µm in all images). Asterisks represent * $P < 0.05$, ** $P < 0.01$, and *** $P < 0.0001$; Error bars represent standard error of mean (SEM).

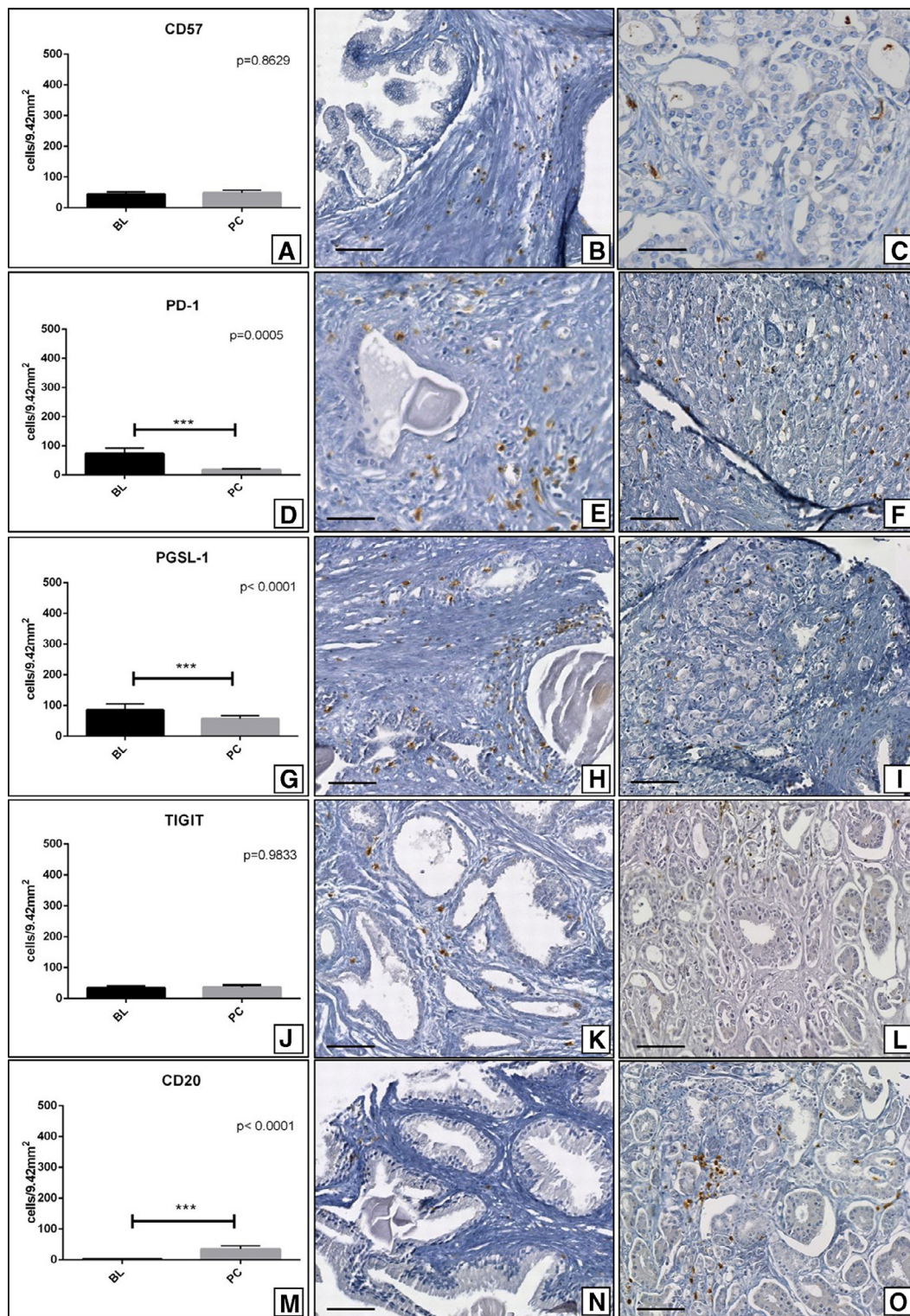


Fig. 2. Evaluation of lymphocyte infiltrate and PTX3 expression in prostate lesions. (A) Graph shows the number of CD57 positive cells in BL and PC lesions. (B) Image displays some CD57 positive inflammatory cells in BL. (C) Representative image of tumor-associate inflammatory CD57 positive cells infiltrate in PC. (D) Graph shows the number of PD-1 positive cells in BL and PC lesions. (E) Several PD-1 positive cells in BL. (F) Rare positive PD-1 positive cells in PC. (G) Graph shows the number of PSGL-1 positive cells in BL and PC lesions. (H) Image shows PSGL-1 positive inflammatory cells in BL. (I) Rare PSGL-1 positive cells in PC. (J) Graph shows the number of TIGIT positive cells in BL and PC lesions. (K) Representative image of tumor-associate inflammatory TIGIT positive cells in BL. (L) Rare positive TIGIT positive cells in PC. (M) Graph shows the number of CD20 positive cells in BL and PC lesions. (N) Image shows numerous CD20 positive inflammatory cells in BL. (O) Numerous CD20 positive cells in PC. (Scale bar represents 200 μ m in all images). Asterisks represent * $P < 0.05$, ** $P < 0.01$ and *** $P < 0.0001$; Error bars represent standard error of mean (SEM).

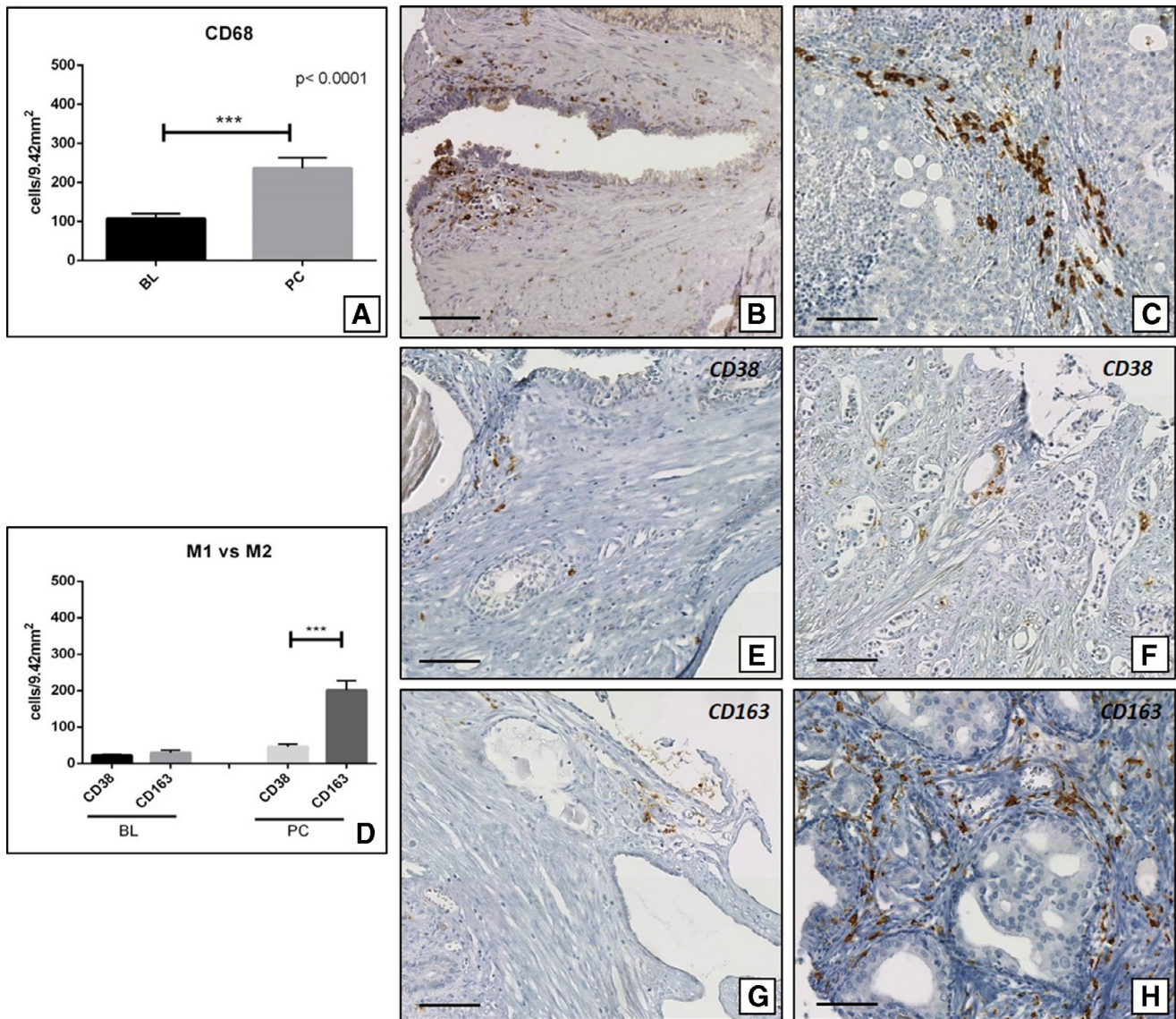


Fig. 3. Evaluation of macrophage infiltrate and PTX3 expression in prostate lesions. (A) Graph shows the number of CD68 positive macrophages in BL and PC lesions. (B) CD68 positive cells in BL. (C) Numerous CD68 positive cells in PC. (D) Graph shows the ratio between M1 (CD38⁺CD3⁻CD20⁻) and M2 (CD 168) macrophages in BL and PC prostate lesions. (E) Image shows CD38 positive cells in BL. (F) Representative image of tumor-associate CD38 positive macrophages in PC. (G) Graph shows the number of CD163 macrophages in BL and PC lesions. (H) No/rare positive CD163 positive macrophages in BL. Asterisks represent * $P < 0.05$, ** $P < 0.01$ and *** $P < 0.0001$; Error bars represent standard error of mean (SEM).

3.6. Correlation between PD-L1 positive cancer cells and inflammatory infiltrate

In order to study the possible correlation between PD-L1 expression and the modifications of inflammatory infiltrate, we subdivided the PC lesions in 3 groups: group A, (lesions with no/rare presence of PD-L1 positive prostate cancer cells: PD-L1 positive prostate cancer cells $< 6/500$), group B (lesions where PD-L1 was expressed by $6 < x < 250/500$ cancer cells), and group C (lesions with more than 250/500 PD-L1 positive prostate cancer cells). Group A represented 54% of PCs, Group B 24% of PCs and Group C 22% of PCs. These results are in line with the main literature studies [30–32]. Indeed, in primary prostate cancers, the

frequency of PD-L1 ranges from 8% to 92% [30–32]. It is important to note that differences in the assessment of PD-L1 expression could include sample processing, antibody selection, and reading scoring system.

3.7. Variations of the inflammatory infiltrate and PTX3 expression related to PD-L1

As concern the number of CD3 intratumoral lymphocytes, we noted an important decrease of these cells in B group as compared with both group A and C (group A: 138.6 ± 32.19 ; group B: 20.00 ± 5.75 ; group C: 40.73 ± 12.21 ; $P = 0.0713$; A vs. B $P = 0.0817$; A vs. C $P = 0.3417$; B vs. C $P = 0.0253$) (Fig. 4A). Also, a significant decrease

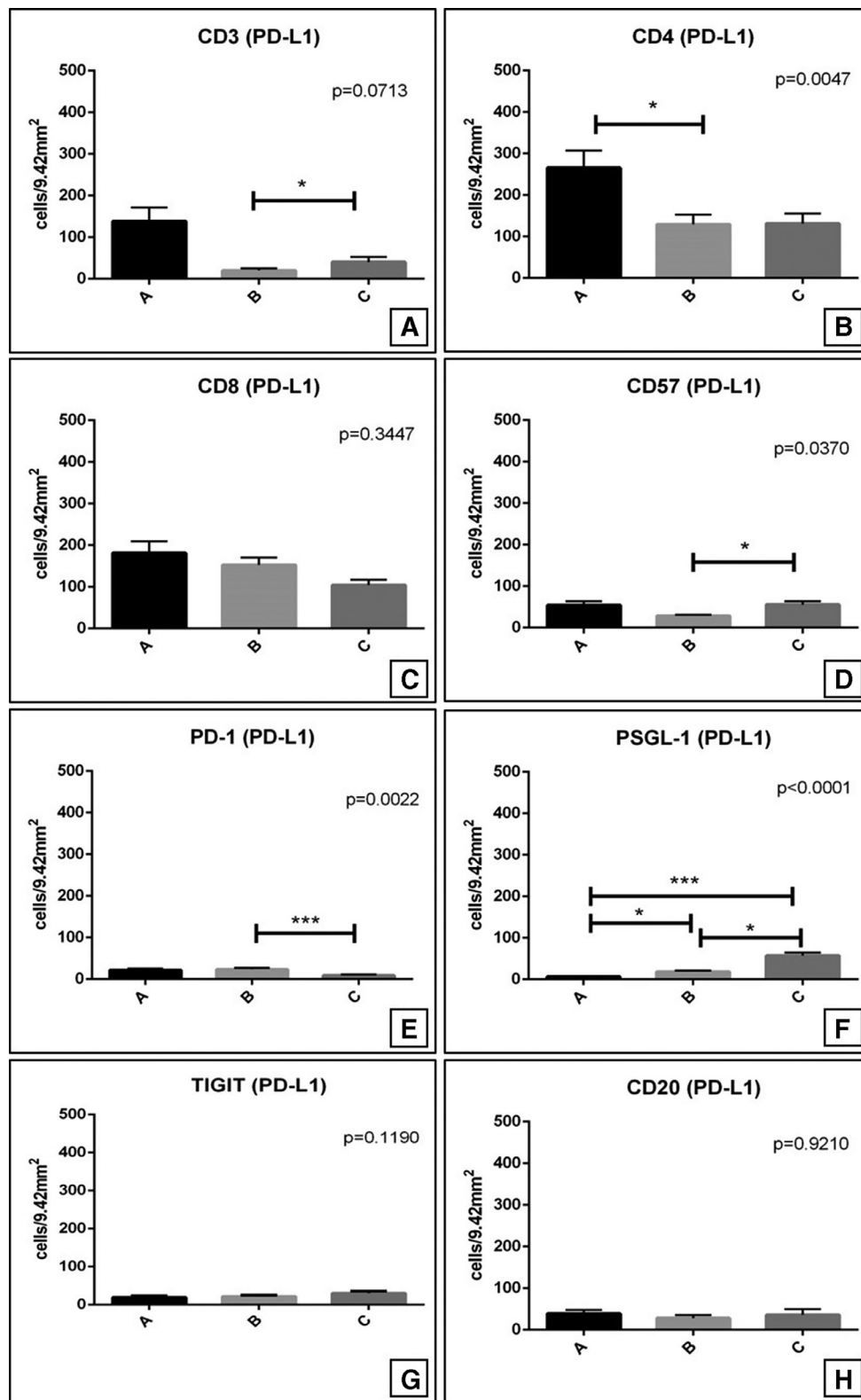


Fig. 4. Variation of lymphocyte tumoral infiltrate related to PD-L1 expression. (A) Graph shows the number of CD3 positive cells in the experimental groups. (B) Graph displays the number of CD4 positive cells in the experimental groups. (C) Graph shows the number of CD8 positive cells in the experimental groups. (D) Graph displays the number of CD57 positive cells in the experimental groups. (E) Graph shows the number of PD-1 positive cells in the experimental groups. (F) Graph displays the number of PSGL-1 positive cells in the experimental groups. (G) Graph shows the number of TIGIT positive cells in the experimental groups. (H) Graph displays the number of CD20 positive cells in the experimental groups. Asterisks represent $*P < 0.05$, $**P < 0.01$ and $***P < 0.0001$; Error bars represent standard error of mean (SEM).

of CD4 lymphocytes was observed in group B as compared group A (group A: 265.7 ± 41.76 , group B: 129.3 ± 23.51 , group C: 131.9 ± 23.50 , $P=0.0047$; A vs. B $P=0.0421$; B vs. C $P=0.7833$; A vs. C $P=0.1094$). No significant differences were observed in regard to the expressions of CD8 (group A: 185.3 ± 28.72 , group B: 152.61 ± 17.55 , group C: 104.5 ± 12.20 , $P=0.3447$; A vs. B $P=0.5479$; B vs. C $P=0.1193$; A vs. C $P=0.5041$) (Fig. 4B and C).

Surprisingly, we observed a reduction of CD57 positive cells only in those carcinomas characterized by the expression of an intermediate number of PD-L1 positive cancer cells (group A: 54.57 ± 9.02 ; group B: 28.63 ± 2.96 ; group C: 55.82 ± 7.85 , $P=0.0370$; A vs. B $P=0.0555$; B vs. C $P=0.3931$; A vs. C $P=0.0132$) (Fig. 4D). A significant decrease of PD-1 positive lymphocytes was observed in prostate lesions of group C (group A: 21.71 ± 3.60 ; group B: 23.70 ± 3.40 ; group C: 9.00 ± 1.90 $P=0.0022$; A vs. B $P=0.1241$; B vs. C $P=0.0001$; A vs. C $P=0.078$) (Fig. 4E). The study of PSGL-1 expression revealed an increase in the number of positive cells in prostate cancer

lesions with higher expression of PD-L1 (group A: 6.37 ± 0.94 ; group B: 18.45 ± 3.19 ; group C: 57.14 ± 7.49 , $P < 0.0001$; A vs. B $P=0.0016$; A vs. C $P < 0.0001$; B vs. C $P=0.0009$) (Fig. 4F). As concern the number of TIGIT positive cells, we did not observe any significant difference comparing them with PD-L1 expression by prostate cancer cells (group A: 19.13 ± 4.40 ; group B: 22.00 ± 3.17 ; group C: 30.00 ± 5.60 $P=0.1190$; A vs. B $P=0.1216$; A vs. C $P=0.0556$; B vs. C $P=0.8216$) (Fig. 4G). Finally, we did not observe correlation between the number of PD-L1 positive cells and the CD20-positive infiltrate (Fig. 4H).

We also observed an inverse correlation between the number of PD-L1 positive cancer cells and PTX3 expression (group A: 436.00 ± 9.57 ; group B: 373.7 ± 23.60 ; group C: 391.8 ± 17.51 , $P=0.0249$; A vs. B $P=0.0407$; B vs. C $P=0.8602$; A vs. C $P=0.0127$) (Fig. 5A).

As concern the study of macrophage populations, for the first time, we reported data about the correlation between PD-L1 expression and the composition of macrophage infiltrate in prostate cancer. Analysis of CD68 displayed a

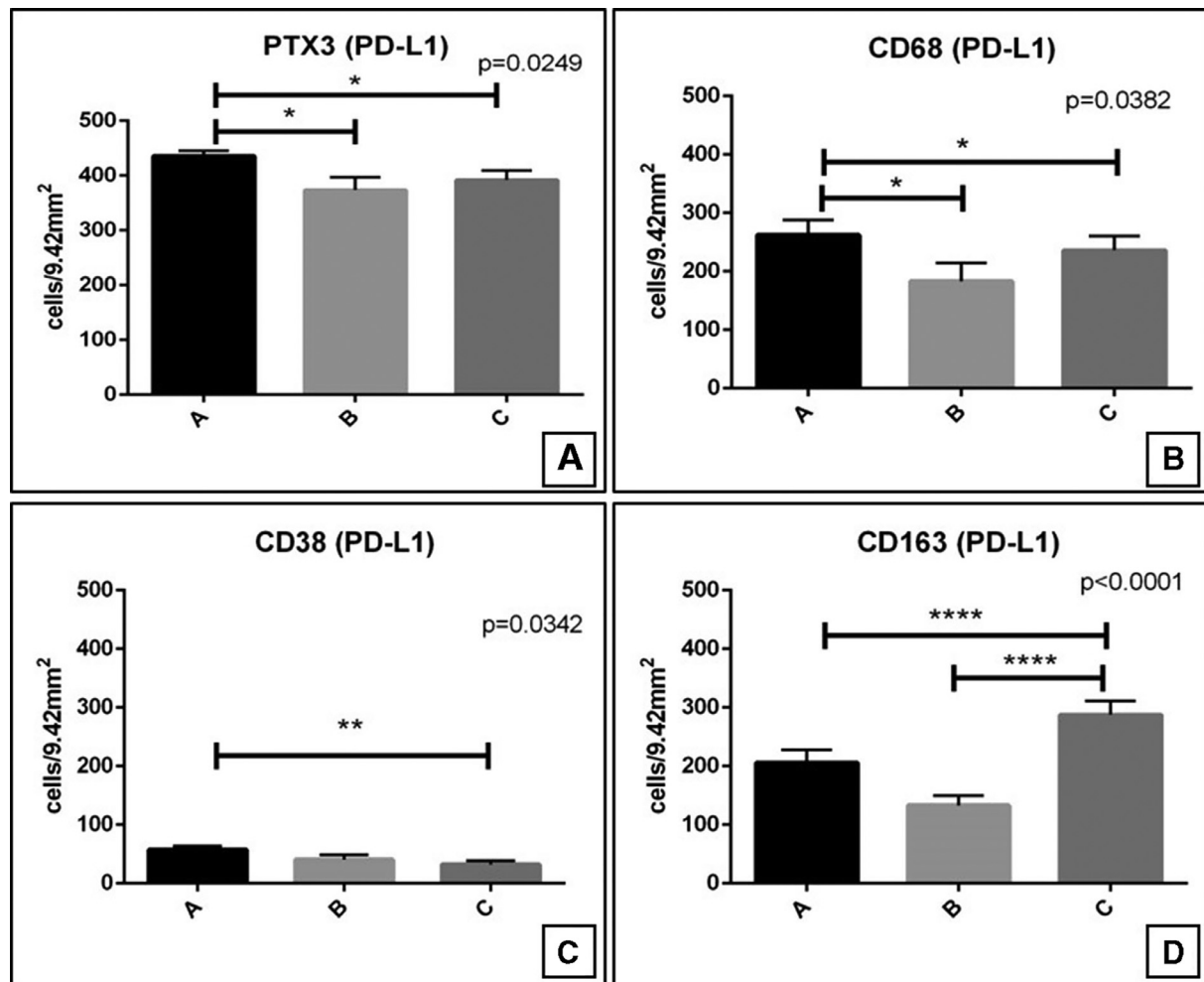


Fig. 5. Variation of macrophage tumoral infiltrate related to PD-L1 expression. (A) Graph shows the number of PTX3 positive cancer cells in the experimental groups. (B) Graph shows the number of CD68 positive macrophages in the experimental groups. (C) Graph displays the number of CD38 positive and CD3-CD20 negative macrophages in the experimental groups. (D) Graph shows the number of CD163 positive macrophages in the experimental groups. Asterisks represent * $P < 0.05$, ** $P < 0.01$ and **** $P < 0.0001$; Error bars represent standard error of mean (SEM).

significant reduction of macrophage intratumoral infiltrate in the group A as compared both with the groups B and C (group A: 262.4 ± 25.34 ; group B: 183.3 ± 31.05 ; group C: 235.91 ± 24.59 , $P = 0.0382$; A vs. B $P = 0.0269$; B vs. C $P = 0.9365$; A vs. C $P = 0.0216$) (Fig. 5B). Noteworthy, analyzing separately the M1 and M2 population we observed a putative association between the number of PD-L1 positive prostate cancer cells and the M2 polarization phenomenon. Indeed, the number of CD38 macrophages (M1) significantly decrease in groups C as compared with group A (group A: 57.71 ± 6.42 ; group B: 40.63 ± 8.42 ; group C: 32.33 ± 6.04 , $P = 0.0342$; A vs. B $P = 0.1532$; B vs. C $P = 0.6832$; A vs. C $P = 0.0075$) (Fig. 5C) whereas we noted that the expression of PD-L1 was associated with the increase of intratumoral CD163 macrophages (M2) (group A: 206.2 ± 21.32 ; group B: 133.1 ± 16.21 ; group C: 287.5 ± 24.12 , $P = 0.0002$; A vs. B $P = 0.0329$; B vs. C $P < 0.0001$; A vs. C $P = 0.0102$) (Fig. 5D).

4. Discussion

Immunological escape is one of the main research topics in the oncological field. To date, it is known that the expression of PD-L1 allows cancer cells to escape the immune response of T lymphocytes, and thus, to trigger the metastatic process in several neoplasms [33–36]. Thus, immunotherapy has become an important cancer treatment modality. Nevertheless, despite the current enthusiasm, such therapeutical approach is probably destined to fail if it is not combined with other drugs. The combination of cancer vaccines or checkpoint inhibitors with different immunotherapeutic agents, hormonal therapy (enzalutamide), radiotherapy (radium 223), DNA-damaging agents (olaparib), or chemotherapy (docetaxel) can enhance immune responses and induce more dramatic, long-lasting clinical responses without significant toxicity [37]. In this context, several immune checkpoint inhibitors have emerged as a new class of drugs capable of enhancing the body's immune response against several different tumor types [38,39]. Immune checkpoint inhibitors approved by the US Food and Drug Administration include monoclonal antibodies against CTLA-4 (ipilimumab [40], PD-1 (nivolumab, [41] pembrolizumab [42]), and, most recently, PD-L1 (atezolizumab [43], avelumab [44], and durvalumab [45]). Additional indications are being explored for approved agents, [46–48] and other immune checkpoint inhibitors are in late-stage development, including a new anti-CTLA-4 antibody (tremelimumab) [49,50]. However, despite these unprecedented successes, most patients experience intrinsic resistance and, even responding patients, can develop acquired resistance to anti-PD-1 or anti-PD-L1 therapy [51]. Numerous studies are currently underway to systematically elucidate the mechanisms underlying this resistance. The presence of intratumoral inflammatory infiltrate associated to the expression of PD-L1 could have a direct, or

indirect, role in the development of anti-PD-1/PD-L1 therapy resistance.

Therefore, in this study, we evaluated the putative correlation between the composition of intratumoral inflammatory infiltrate and the expression of PD-L1 by prostate cancer. Inflammatory infiltration was evaluated both in relation to the type of prostatic lesion (BL vs. PC) and to the expression of PD-L1. In particular, to evaluate the influence of PD-L1 in the composition of the inflammatory population, PCs were divided into 3 subgroups (i.e. low, intermediate, and high number of PD-L1 positive cancer cells). In line with the literature, we observed a frequent expression of PD-L1 in neoplastic prostate cells [52]. To evaluate the differences in the inflammatory infiltrate, we investigated molecular markers able to highlight the presence of the main immune cells. Specifically, the total T-lymphocyte population, CD3 positive lymphocytes was studied. T lymphocytes are involved in the effector response capable of eliminating tumor cells [53]. The total lymphocyte population is composed of CD4-positive T lymphocytes and CD8 lymphocytes. CD4-positive lymphocytes generally perform their antitumor activity by stimulating T-cell division, differentiation to effector T cells and, in the case of B lymphocytes, the antibodies synthesis [53]. Furthermore, CD4 positive cells are able to potentiate the activation of macrophages, helping them to destroy cancer cells [53]. On the other hand, CD8-positive T lymphocytes can act on cancer cells releasing proteins (known as perforins) that forms a pore in the cell membrane determining its destruction [53]. As already reported by Buisseret et al. [54], in this work it was observed an increase in CD4+ T lymphocytes in PCs. The CD4 lymphocytes response is present to counteract tumor progression but unexpectedly no differences were observed with respect to the number of CD8+ lymphocytes. By evaluating the changes in the T CD4 / CD8 population in relation to PD-L1 positive cancer cells, we demonstrated that the expression of this molecule was associated with a decrease of CD4+ inflammatory infiltrate. As expected, the number of PD1 positive lymphocytes decreased in the prostate lesions characterized by a number of PD-L1 positive cells $> 250/500$. Recently, it has been highlighted the role of PSGL-1 as an immune checkpoint regulator that promotes T-cell exhaustion [55]. Specifically, in cancer environment it has been found that PSGL-1-deficiency enhanced T-cell antitumor immunity to melanoma [56]. In line with these data, for the first time, we reported a putative correlation between the expression of PD-L1 by prostate cancer cells and the presence of PSGL-1 positive intratumoral inflammatory infiltrate. This can suggest an involvement of PSGL-1 in the complex mechanism of immune-escape of prostate cancer.

In the onco-immunity field, the role of tumor-associated macrophages, or TAMs, has recently gained great importance, since these can contribute to tumor progression, by promoting genetic instability and supporting metastasis. Furthermore, TAMs play a fundamental role in the response

to cytoreductive therapy (chemotherapy and radiotherapy), where they can antagonize the antitumoral activity of these treatments [57,58]. Today, TAMs are considered sensitive therapeutic targets for immunomodulation of the tumor microenvironment. In this context, has been proposed that the M2 with an anti-inflammatory effect can have a protumor effect in numerous neoplasms [59,60]. Here we showed a putative relationship between tumoral PD-L1 expression and changes in macrophage response. These data showed that, in prostate tumors characterized by numerous positive PD-L1 cells, there is a reduction of the macrophage tumor population characterized by a prevalent presence of M2 polarized residual macrophages. The reduction and M2 polarization of macrophages, linked to the expression of PD-L1, represents another element supporting the negative prognostic value of this molecule.

To better characterize the inflammatory response associated with prostatic lesions, it has been investigated the expression of an inflammation-associated molecule: PTX3. Recent studies have shown that PTX3 may have a prooncogenic role in some cancers, including ovary and lung cancer, prostate carcinoma, pancreatic carcinoma, and bone metastasis from breast cancer [61-63]. However, some studies report a protective role of PTX3 against cancer [64]. Reports showing a positive correlation between PTX3 expression and poor prognosis in specific human tumors suggest that the role of PTX3 may be very dependent on tissue, cancer type and from the cellular source [62-64]. Our results showed an over-expression of PTX3 in PCs, compared to BL, suggesting therefore its possible involvement in tumor progression. In addition, PTX3 could play a role in inflammatory tumor-associated response; indeed, we noted a significant inverse correlation between its expression by prostate tumor cells and the number of PD-L1 positive cells.

The results reported in this study allowed to characterize the inflammatory population associated with prostate tumorigenesis. Furthermore, for the first time the cellular inflammatory pattern associated with PD-L1 expression was defined, in particular for the macrophage population. To date, in fact, there is still no data in literature reporting the association between PD-L1 expression and changes in the intratumoral macrophage population.

5. Conclusions

Data here reported highlighted new aspects about the relationship between PD-L1 expression by prostate cancer cells and the composition of tumor-associated inflammatory infiltrate, especially for macrophages populations. If confirmed, our data can be useful to develop therapeutical strategies able to inhibit the PD-L1 activity and, at the same time, to re-activate the antitumor inflammatory process.

In the advancing field of cancer immunotherapy, the antibody based-positron emission tomography (immune-PET) constitutes an exciting and expanding noninvasive

option that not simply improves diagnostic tumor characterization but also help in the monitoring of cancer immune-response [65,66]. In this context, the use of Zirconium-89 as a PET surrogate radioisotope for in vivo scouting of therapeutic ^{90}Y or ^{117}Lu -labeled antibodies could allow to individuate the best radio-immunotherapy dose schedules for patients, and also to develop new therapeutical protocols for the immune-modulation of intratumoral inflammatory infiltrate.

Disclosure

There are no potential conflicts of interest relating to the manuscript (for each author), and there were no extramural sources supporting this research (excluding sources already declared). The study is original and the manuscript has not been published yet and is not being considered for publication elsewhere in any language either integrally or partially except as an abstract. All authors have agreed with the submission in its present (and subsequent) forms.

Acknowledgments

Authors wish to thank Dr. Sara Ciuffa, Dr. Harpreet Kaur Lamsira, and OrchideaLab S.r.l for technical support. Anti-TIGIT antibody was kindly provided by UCS diagnostic S.r.l.

Supplementary materials

Supplementary material associated with this article can be found in the online version at <https://doi.org/10.1016/j.urolonc.2019.02.013>.

References

- [1] Ferlay J, Soerjomataram I, Dikshit R, Eser S, Mathers C, Rebelo M, et al. Cancer incidence and mortality worldwide: sources, methods and major patterns in GLOBOCAN 2012. *Int J Cancer* 2015 Mar 1;136(5):E359–86.
- [2] Thompson I, Thrasher JB, Aus G, Burnett AL, Canby-Hagino ED, Cookson MS, et al. Guideline for the management of clinically localized prostate cancer: 2007 update. *J Urol* 2007 Jun;177(6):2106–31.
- [3] Kim EH, Bullock AD. Surgical management for prostate cancer. *Mo Med* 2018 Mar-Apr;115(2):142–5.
- [4] Virgo KS, Basch E, Loblaw DI, Oliver TK, Rumble RB, Carducci MA, et al. Second-line hormonal therapy for men with chemotherapy-naïve, castration-resistant prostate cancer: American society of clinical oncology provisional clinical opinion. *J Clin Oncol* 2017 Jun 10;35(17):1952–64.
- [5] de Bono JS, Oudard S, Ozguroglu M, Hansen S, Machiels JP, Kocak I, et al. Prednisone plus cabazitaxel or mitoxantrone for metastatic castration-resistant prostate cancer progressing after docetaxel treatment: a randomised open-label trial. *Lancet* 2010 Oct 2;376(9747):1147–54.
- [6] Ryan CJ, Smith MR, Fizazi K, Saad F, Mulders PF, Sternberg CN. Abiraterone acetate plus prednisone versus placebo plus prednisone in chemotherapy-naïve men with metastatic castration-resistant prostate cancer (COU-AA-302): final overall survival analysis of a

- randomised, double-blind, placebo-controlled phase 3 study. *Lancet Oncol* 2015 Feb;16(2):152–60.
- [7] Beer TM, Tombal B. Enzalutamide in metastatic prostate cancer before chemotherapy. *N Engl J Med* 2014 Oct 30;371(18):1755–6.
- [8] Modena A, Ciccarese C, Iacovelli R, Brunelli M, Montironi R, Fiorentino M, et al. Immune checkpoint inhibitors and prostate cancer: a new frontier? *Oncol Rev* 2016 Apr 15;10(1):293.
- [9] Hanahan D, Weinberg RA. Hallmarks of cancer: the next generation. *Cell* 2011 Mar 4;144(5):646–74.
- [10] Black M, Barsoum IB, Truesdell P, Cotechini T, Macdonald-Goodfellow SK, Petroff M, et al. Activation of the PD-1/PD-L1 immune checkpoint confers tumour cell chemoresistance associated with increased metastasis. *Oncotarget* 2016 Mar 1;7(9):10557–67.
- [11] Iwai Y, Ishida M, Tanaka Y, Okazaki T, Honjo T, Minato N. Involvement of PD-L1 on tumour cells in the escape from host immune system and tumour immunotherapy by PD-L1 blockade. *Proc Natl Acad Sci USA* 2002 Sep 17;99(19):12293–7.
- [12] Zang X, Allison JP. The B7 family and cancer therapy: costimulation and coinhibition. *Clin Cancer Res* 2007 Sep 15;13(18 Pt 1):5271–9.
- [13] Breviario F, d'Aniello EM, Golay J, Peri G, Bottazzi B, Bairoch A, et al. Interleukin-1-inducible genes in endothelial cells. Cloning of a new gene related to C-reactive protein and serum amyloid P component. *J Biol Chem* 1992;267:22190–7.
- [14] Moalli F, Jaillon S, Inforzato A, Sironi M, Bottazzi B, Mantovani A, et al. Pathogen recognition by the long pentraxin PTX3. *J Biomed Biotechnol* 2011;2011:830421.
- [15] Chorny A, Casas-Recasens S, Sintès J, Shan M, Polentarutti N, Garcia-Escudero R, et al. The soluble pattern recognition receptor PTX3 links humoral innate and adaptive immune responses by helping marginal zone B cells. *J Exp Med* 2016;213:2167–85.
- [16] Chang WC, Wu SL, Huang WC, Hsu JY, Chan SH, Wang JM, et al. PTX3 gene activation in EGF-induced head and neck cancer cell metastasis. *Oncotarget* 2015;6:7741–57.
- [17] Choi B, Lee EJ, Shin MK, Park YS, Ryu MH, Kim SM, et al. Upregulation of brain-derived neurotrophic factor in advanced gastric cancer contributes to bone metastatic osteolysis by inducing long pentraxin 3. *Oncotarget* 2016;7:55506–17.
- [18] Scimeca M, Antonacci C, Toschi N, Giannini E, Bonfiglio R, Buonomo CO, et al. Breast osteoblast-like cells: a reliable early marker for bone metastases from breast cancer. *Clin Breast Cancer* 2018 Aug;18(4):e659–69.
- [19] Choi B, Lee EJ, Song DH, Yoon SC, Chung YH, Jang Y, et al. Elevated Pentraxin 3 in bone metastatic breast cancer is correlated with osteolytic function. *Oncotarget* 2014;5:481–92.
- [20] Locatelli M, Ferrero S, Martinelli Boneschi F, Boiocchi L, Zavanone M, Maria Gaini S, et al. The long pentraxin PTX3 as a correlate of cancer-related inflammation and prognosis of malignancy in gliomas. *J Neuroimmunol* 2013;260:99–106.
- [21] Stallone G, Cormio L, Netti GS, Infante B, Selvaggio O, Fino GD, et al. Pentraxin 3: a novel biomarker for predicting progression from prostatic inflammation to prostate cancer. *Cancer Res* 2014;74:4230–8.
- [22] Scimeca M, Urbano N, Rita B, Mapelli SN, Catapano CV, Carbone GM, et al. Prostate osteoblast-like cells: a reliable prognostic marker of bone metastasis in prostate cancer patients. *Contrast Media Mol Imaging* 2018 Dec 9;2018:9840962.
- [23] Diamandis EP, Goodglick L, Planque C, Thornquist MD. Pentraxin-3 is a novel biomarker of lung carcinoma. *Clin Cancer Res* 2011 Apr 15;17(8):2395–9.
- [24] Ronca R, Giacomini A, Di Salle E, Coltrini D, Pagano K, Ragona L, et al. Long-pentraxin 3 derivative as a small-molecule FGF trap for cancer therapy. *Cancer Cell* 2015;28:225–39.
- [25] Wang JX, He YL, Zhu ST, Yang S, Zhang ST. Aberrant methylation of the 3q25 tumour suppressor gene PTX3 in human esophageal squamous cell carcinoma. *World J Gastroenterol* 2011;17:4225–30.
- [26] Tafani M, Di Vito M, Frati A, Pellegrini L, De Santis E, Sette G, et al. Pro-inflammatory gene expression in solid glioblastoma microenvironment and in hypoxic stem cells from human glioblastoma. *J Neuroinflamm* 2011;32:1–16.
- [27] De Luca A, Rotili D, Carpanese D, Lenoci A, Calderan L, Scimeca M, et al. A novel orally active water-soluble inhibitor of human glutathione transferase exerts a potent and selective antitumour activity against human melanoma xenografts. *Oncotarget* 2015 Feb 28;6(6):4126–43.
- [28] Scimeca M, Giannini E, Antonacci C, Pistolesse CA, Spagnoli LG, Bonanno E. Microcalcifications in breast cancer: an active phenomenon mediated by epithelial cells with mesenchymal characteristics. *BMC Cancer* 2014 Apr 23;14:286.
- [29] Mottet N, Bellmunt J, Bolla M, Briers E, Cumberbatch MG, De Santis M, et al. EAU-ESTRO-SIOG guidelines on prostate cancer. Part 1: screening, diagnosis, and local treatment with curative intent. *Eur Urol* 2017 Apr;71(4):618–29.
- [30] Haffner MC, Guner G, Taheri D, Netto GJ, Palsgrove DN, Zheng Q, et al. Comprehensive evaluation of programmed death-ligand 1 expression in primary and metastatic prostate cancer. *Am J Pathol* 2018 Jun;188(6):1478–85.
- [31] Calagua C, Russo J, Sun Y, Schaefer R, Lis R, Zhang Z, et al. Expression of PD-L1 in hormone-naïve and treated prostate cancer patients receiving neoadjuvant abiraterone acetate plus prednisone and leuprolide. *Clin Cancer Res* 2017 Nov 15;23(22):6812–22.
- [32] Baas W, Gershburg S, Dynda D, Delfino K, Robinson K, Nie D, et al. Immune characterization of the programmed death receptor pathway in high risk prostate cancer. *Clin Genitourin Cancer* 2017 Oct;15(5):577–81.
- [33] Bonfiglio R, Nardozi D, Scimeca M, Cerroni C, Mauriello A, Bonanno E. PD-L1 in immune-escape of breast and prostate cancers: from biology to therapy. *Future Oncol* 2017 Oct;13(24):2129–31.
- [34] Zhang M, Sun H, Zhao S, Wang Y, Pu H, Wang Y, et al. Expression of PD-L1 and prognosis in breast cancer: a meta-analysis. *Oncotarget* 2017 May 9;8(19):31347–54.
- [35] Somasundaram A, Burns TF. The next generation of immunotherapy: keeping lung cancer in check. *J Hematol Oncol* 2017 Apr 24;10(1):87.
- [36] Motz GT, Coukos G. Deciphering and reversing tumour immune suppression. *Immunity* 2013 Jul 25;39(1):61–73.
- [37] Bilusic M, Madan RA, Gulley JL. Immunotherapy of prostate cancer: facts and hopes. *Clin Cancer Res* 2017 Nov 15;23(22):6764–70.
- [38] Larkin J, Chiarion-Sileni V, Gonzalez R, Grob JJ, Cowey CL, Lao CD, et al. Combined nivolumab and ipilimumab or monotherapy in untreated melanoma. *N Engl J Med* 2015;373(1):23–34.
- [39] Davies M, Duffield EA. Safety of checkpoint inhibitors for cancer treatment: strategies for patient monitoring and management of immune-mediated adverse events. *Immunotargets Ther* 2017 Aug 24;6:51–71.
- [40] Bristol-Myers Squibb Company. Yervoy® (ipilimumab) Injection [prescribing information]. Princeton, NJ: Bristol-Myers Squibb Company; 2017.
- [41] Bristol-Myers Squibb Company. Opdivo® (nivolumab) injection [prescribing information]. Princeton, NJ: Bristol-Myers Squibb Company; 2017.
- [42] Merck & Company Inc. Keytruda® (pembrolizumab) for injection [prescribing information]. Whitehouse Station, NJ: Merck & Co Inc; 2017.
- [43] Genentech Inc. Tecentriq® (atezolizumab) injection [prescribing information]. South San Francisco, CA: Genentech, Inc; 2017.
- [44] EMD Serono Inc. Bavencio® (avelumab) injection, for intravenous use [prescribing information]. Rockland, MD: EMD Serono, Inc. and Pfizer, Inc; 2017.
- [45] AstraZeneca Pharmaceuticals LP. Imfinzi™ (durvalumab) injection, for intravenous use [prescribing information]. Wilmington, DE: AstraZeneca Pharmaceuticals LP; 2017.
- [46] Nanda R, Chow LQ, Dees EC, Berger R, Gupta S, Geva R, et al. Pembrolizumab in patients with advanced triple-negative breast cancer: phase Ib KEYNOTE-012 study. *J Clin Oncol* 2016;34(21):2460–7.

- [47] Tang J, Yu JX, Hubbard-Lucey VM, Neftelinov ST, Hodge JP, Lin Y. Trial watch: the clinical trial landscape for PD1/PDL1 immune checkpoint inhibitors. *Nat Rev Drug Discov* 2018 Nov 28;17(12):854–5.
- [48] Antonia SJ, López-Martin JA, Bendell J, Ott PA, Taylor M, Eder JP, et al. Nivolumab alone and nivolumab plus ipilimumab in recurrent small-cell lung cancer (CheckMate 032): a multicentre, open-label, phase 1/2 trial. *Lancet Oncol* 2016;17(7):883–95.
- [49] Ribas A, Hanson DC, Noe DA, Millham R, Guyot DJ, Bernstein SH, et al. Tremelimumab (CP-675,206), a cytotoxic T lymphocyte associated antigen 4 blocking monoclonal antibody in clinical development for patients with cancer. *Oncologist* 2007;12(7):873–83.
- [50] National Comprehensive Cancer Network Small Cell Lung Cancer (v3.2017) 2017. [Accessed March 15, 2017]. Available from: https://www.nccn.org/professionals/physician_gls/pdf/sclc.pdf.
- [51] Sharma P, Hu-Lieskovan S, Wargo JA, Ribas A. Primary, adaptive, and acquired resistance to cancer immunotherapy. *Cell* 2017;168:707–23.
- [52] Papanicolau-Sengos A, Yang Y, Pabla S, Lenzo FL, Kato S, Kurzrock R, et al. Identification of targets for prostate cancer immunotherapy. *Prostate* 2019 Jan 6. <https://doi.org/10.1002/pros.23756>.
- [53] Parkin J, Cohen B. An overview of the immune system. *Lancet* 2001 Jun 2;357(9270):1777–89.
- [54] Buisseret L, Garaud S, de Wind A, Van den Eynden G, Boisson A, Solinas C, et al. Tumour-infiltrating lymphocyte composition, organization and PD-1/ PD-L1 expression are linked in breast cancer. *Oncoimmunology* 2016 Dec 14;6(1):e1257452.
- [55] Tinoco R, Carrette F, Barraza ML, Otero DC, Magaña J, Bosenberg MW, et al. PSGL-1 is an immune checkpoint regulator that promotes T cell exhaustion. *Immunity* 2016 May 17;44(5):1190–203.
- [56] Tinoco R, Otero DC, Takahashi AA, Bradley LM. PSGL-1: a new player in the immune checkpoint landscape. *Trends Immunol* 2017 May;38(5):323–35.
- [57] Erlandsson A, Carlsson J, Lundholm M, Fält A, Andersson SO, Andrén O, et al. M2 macrophages and regulatory T cells in lethal prostate cancer. *Prostate* 2019 Mar;79(4):363–9.
- [58] Mantovani A, Marchesi F, Malesci A, Laghi L, Allavena P. Tumour-associated macrophages as treatment targets in oncology. *Nat Rev Clin Oncol* 2017 Jul;14(7):399–416.
- [59] Galdiero MR, Garlanda C, Jaillon S, Marone G, Mantovani A. Tumour associated macrophages and neutrophils in tumour progression. *J Cell Physiol* 2013 Jul;228(7):1404–12.
- [60] Suarez-Lopez L, Sriram G, Kong YW, Morandell S, Merrick KA, Hernandez Y, et al. MK2 contributes to tumour progression by promoting M2 macrophage polarization and tumour angiogenesis. *Proc Natl Acad Sci USA* 2018 May 1;115(18):E4236–44.
- [61] Daigo K, Mantovani A, Bottazzi B. The yin-yang of long pentraxin PTX3 in inflammation and immunity. *Immunol Lett* 2014 Sep;161(1):38–43.
- [62] Bonavita E, Gentile S, Rubino M, Maina V, Papait R, Kunderfranco P, et al. PTX3 is an extrinsic oncosuppressor regulating complement-dependent inflammation in cancer. *Cell* 2015 Feb 12;160(4):700–14.
- [63] Bonfiglio R, Scimeca M, Toschi N, Pistolese CA, Giannini E, Antonacci C, et al. Radiological, histological and chemical analysis of breast microcalcifications: diagnostic value and biological significance. *J Mammary Gland Biol Neoplasia* 2018 Jun;23(1-2):89–99.
- [64] Giacomini A, Ghedini GC, Presta M, Ronca R. Long pentraxin 3: a novel multifaceted player in cancer. *Biochim Biophys Acta* 2018 Jan;1869(1):53–63.
- [65] Scimeca M, Urbano N, Bonfiglio R, Schillaci O, Bonanno E. Management of oncological patients in the digital era: anatomic pathology and nuclear medicine teamwork. *Future Oncol* 2018 May;14(11):1013–5.
- [66] Urbano N, Scimeca M, Bonanno E, Schillaci O. Nuclear medicine and anatomic pathology in personalized medicine: a challenging alliance. *Per Med*. 2018 Nov;15(6):457–9.
- [67] Scimeca M, Salustri A, Bonanno E, Nardozi D, Rao C, Piccirilli E, et al. Impairment of PTX3 expression in osteoblasts: a key element for osteoporosis. *Cell Death Dis* 2017 Oct 12;8(10):e3125.